

## Dichroism in Ag nanoparticle composites with bimodal size distribution

R. H. Magruder III,<sup>1,a)</sup> S. J. Robinson,<sup>1</sup> C. Smith,<sup>1</sup> A. Meldrum,<sup>2</sup> A. Halabica,<sup>3</sup> and R. F. Haglund, Jr.<sup>3,b)</sup>

<sup>1</sup>Department of Chemistry and Physics, Belmont University, Nashville, Tennessee 37212, USA

<sup>2</sup>Department of Physics, University of Alberta, Edmonton AB T6G 2J1, Canada

<sup>3</sup>Department of Physics and Astronomy, Vanderbilt University, Nashville, Tennessee 37235, USA

(Received 21 October 2008; accepted 1 December 2008; published online 21 January 2009)

We measured the reflectivity of nanoparticle thin films with bimodal size distributions clearly separated by depth and found distinctive spectral differences depending on the direction of illumination. In contrast with previous experiments that implied such differences, the samples in this experiment are prepared by ion implantation at sufficiently high energy to achieve the necessary spatial separation between larger and smaller nanoparticles. We demonstrate that the difference between scattering and absorption probabilities as a function of nanoparticle size is responsible for the differences in maximum reflectivities as the direction of illumination is reversed. This conjecture is supported by a Mie scattering calculation. © 2009 American Institute of Physics.

[DOI: 10.1063/1.3065531]

### I. INTRODUCTION

It has been known for centuries that glasses loaded with metal nanoparticles (NPs) may exhibit different colors, depending on whether or not they are viewed in transmission or reflection. The Lycurgus cup in the British Museum is perhaps the most famous example of the phenomenon.<sup>1</sup> Nistor *et al.*<sup>2</sup> observed a related phenomenon in the reflection spectra from Ag nanocrystals formed in silicate glass cover slips by ion implantation: the peak reflected wavelength varied depending on whether the implanted (front) versus the non-implanted (back) face of the sample was illuminated. These authors noted the hint of several peaks in the reflected spectrum, possibly due to the difference in scattering versus extinction probabilities for large and small NPs. However, the shift in peak wavelength of reflectivity between the front and back side measurements was small ( $\sim 10$  nm) and the line-widths were so large that it is difficult to tell whether or not the difference results simply from the broad size distribution of the NPs or from real differences in the scattering behavior. Moreover, effects due to the complex structure and composition of the silicate glass may also have been in play, further complicating the interpretation of the results.

A significant difference in the front-versus back-side reflectivity as a function of wavelength suggests unique device applications controlled by directionally dependent differences in plasmonic responses. For instance, one can imagine dichroic mirrors in which the reflectivity depends not only on wavelength but also on the propagation direction. Another possibility would be Fabry–Pérot resonators in which the resonance wavelength would depend on the direction from which the light enters the device. In the experiments reported here, we take advantage of improved control of implantation and material parameters to demonstrate the possibility of

controlling this bimodal reflectivity behavior and describe the necessary conditions for systematically designing and preparing such materials.

The model material system for our demonstration comprises Ag NPs prepared by ion implantation in fused silica, where the silver is known to form nanocrystals even without annealing.<sup>2–4</sup> The size of the NPs is a function of dose, dose rate, and substrate temperature for a given implantation energy.<sup>5,6</sup> Ag also is unique among the noble metals in that it has strong interband transitions in the visible.<sup>7</sup> This makes it a useful demonstration material for the purpose of uncovering the underlying optical physics.

### II. EXPERIMENT AND RESULTS

Type III silica samples (Corning 7940) were implanted sequentially with Ag ions at 305 keV. Ag was implanted with fluences of 3.0, 4.5, and  $6 \times 10^{16}$  ions/cm<sup>2</sup> at an average current density of 5  $\mu$ A/cm<sup>2</sup>; these samples are labeled as 3 Ag, 4.5 Ag, and 6 Ag in the narrative that follows. In all the cases substrates were held at  $\sim 0$  °C during the implantations using a thermoelectric cooler. Figure 1 shows the depth distribution of the Ag for a typical sample, measured by Rutherford backscattering (RBS) using 2 MeV He<sup>+</sup> ions.

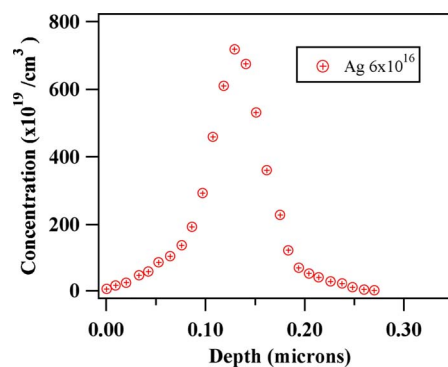


FIG. 1. (Color online) The depth distribution of Ag atoms in the 6 Ag sample measured by RBS.

<sup>a)</sup>Also at Department of Electrical Engineering and Computer Science, Vanderbilt University, Nashville, TN 37235, USA.

<sup>b)</sup>Electronic mail: richard.haglund@vanderbilt.edu.

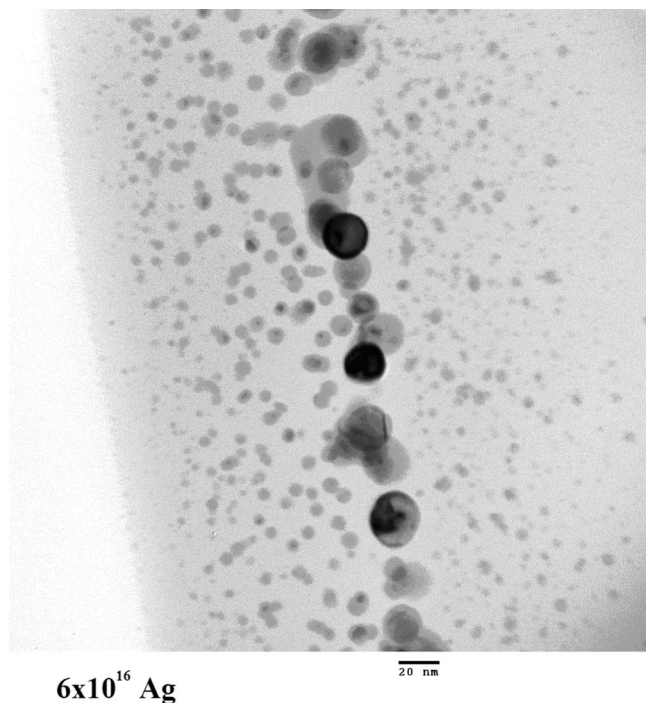


FIG. 2. Cross-sectional TEM image of the 6 Ag sample.

The microstructure of NPs in these composite materials was characterized by transmission electron microscopy (TEM). Samples were prepared by standard cross-section thinning techniques and were analyzed in a JOEL 2010 TEM equipped with a LaB<sub>6</sub> filament. Figure 2 shows a typical cross-sectional TEM micrograph for the 6 Ag sample. From the TEM results the larger NPs occur in a band surrounded by smaller particles located at both shallower and deeper regions, as has been previously reported.<sup>8</sup> As can be seen in the figure, the largest number of small particles is on the side of the larger band nearer the implanted surface, consistent with the Ag depth profile shown in Fig. 1.

The high degree of overlapping in the images, due to the overall specimen thickness, made the generation of size-distribution histograms and number density counts quite difficult. Such distributions were also found to be somewhat misleading visually since although the band of large particles accounts for only a small fraction of the total number of NPs, it still represents a major fraction of the net volume of nanoparticulate Ag. The cluster number density (i.e., number of clusters per unit volume) is also difficult to obtain by TEM due to specimen-to-specimen variations in thickness; however, the 4.5 Ag and 6 Ag samples consistently exhibited a relatively larger number of smaller NPs nearer the implanted surface. Qualitatively one observes that the larger NPs in the 6 Ag sample are roughly 20 nm in diameter, while the smaller NPs are closer to 5 nm in diameter; for the 3 Ag and 4.5 Ag samples, we can expect modest reductions in the diameters of both larger and smaller NPs.

Optical measurements were made at room temperature in air from 900 to 200 nm at wavelength intervals of 1 nm using a Cary 5 dual-beam spectrometer with an unimplanted sample in the reference beam and a spot size of 0.15 cm<sup>2</sup>. All absorption measurements represent the difference be-

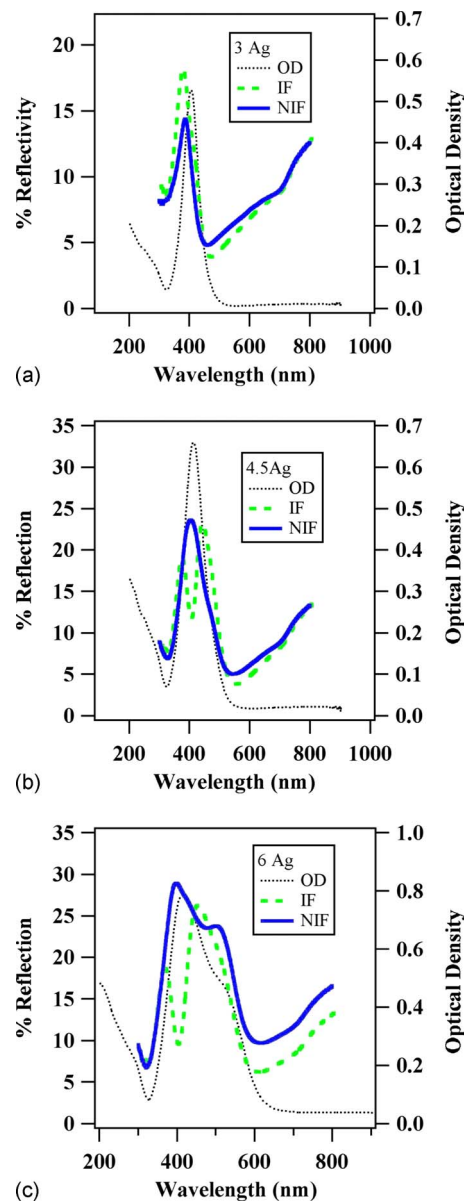


FIG. 3. (Color online) Optical IF and NIF reflectance and absorption (optical density) spectra of (a) 3 Ag, (b) 4:5 Ag, and (c) 6 Ag samples.

tween implanted and unimplanted samples and are reported in units of optical density. The absorption was measured at three different positions on the sample; the scatter in the absorption from varying the measurement position was less than  $\pm 3\%$ , while the point-to-point relative variation (i.e., noise) in the data was less than  $\pm 2\%$ .

The relative reflectance measurements were made using a Harrick Model ERA-12G reflectance attachment in the dual-beam spectrophotometer. Employing single-beam mode with a silvered mirror for normalization, the reflectance spectra were measured from 800 to 300 nm in 1 nm increments. The sampling area for the reflectance measurements was 0.07 cm<sup>2</sup>. Each sample was measured at three different positions. There is less than 5% variance in the spectra due to position, while the rms noise in the spectral data was less than  $\pm 2\%$ .

Figure 3 shows the reflectances and optical densities measured on the implanted (IF) and nonimplanted (NIF)

TABLE I. Peaks in reflectance and absorption measurements.

Sample	Reflectance peaks (nm)	OD peaks (nm)
3 Ag IF	370	402
3 Ag NIF	384	402
4.5 Ag IF	370, 439	410
4.5 Ag NIF	404	410
6 Ag IF	365, 449 <sup>a</sup>	412
6 Ag NIF	398 <sup>b</sup>	412

<sup>a</sup>Shoulder at 502 nm.<sup>b</sup>Shoulder at 503 nm.

faces for all three samples. A peak at 370 nm is observed in the IF reflection spectrum, while in the NIF reflectance spectrum the peak reflectance is redshifted to 384 nm. The optical density has a surface plasmon resonance (SPR) peak at 402 nm, dominated by the larger particles.

Figure 3(b) shows the IF and NIF reflectances and the optical density for the 4.5 Ag sample. In the IF reflectance spectra the 4.5 Ag sample has peaks at 370 and 439 nm; the NIF reflectance spectrum has a peak at 404 nm, while the optical density exhibits a peak at 410 nm.

The IF and NIF reflectances and optical density for the 6 Ag sample are shown in Fig. 3(c). The IF spectrum shows peaks at 365 and 449 nm, with a shoulder at  $\sim 502$  nm, while the NIF spectrum has a single peak at 391 nm and a second incipient peak at  $\sim 503$  nm. This last feature could be a higher-order multipole reflectance peak or, more likely, given the size of the larger NPs, a dipole-dipole interaction manifest in reflection. The absorption spectrum for the 6 Ag sample has a peak at  $\sim 412$  nm (Ref. 9) and shoulder at  $\sim 524$  nm with increasing absorption for wavelengths less than  $\sim 310$  nm, similar to all the other samples. The spectral features of all three samples are summarized in Table I.

### III. DISCUSSION

The Ag samples exhibit absorption feature characteristics of the formation of Ag NPs and the optical response associated with the localized SPR (LSPR).<sup>10-12</sup> For modest NP concentrations, the absorption spectra can be described using effective medium theory for spherical nanometer dimension metal particles embedded in a dielectric.<sup>13</sup> The absorption coefficient  $\alpha$  for noninteracting NPs with diameters less than  $\sim 25$  nm in the electric-dipole approximation<sup>14</sup> is given by

$$\alpha = \frac{18\pi n_d^3 p \epsilon_2}{\lambda [\epsilon_1 + 2n_d^2]^2 + \epsilon_2^2}, \quad (1)$$

where  $\epsilon(\lambda) = \epsilon_1 + i\epsilon_2$  is the complex dielectric constant of the metal,  $p$  is the volume fraction occupied by the metal NPs, and  $n_d$  is the index of refraction of the dielectric host. The frequency-dependent dielectric function  $\epsilon_1$  is negative for metals in the Drude model throughout the frequency range  $\omega < \omega_p$ , where  $\omega_p$  is the plasma frequency. The absorption exhibits a peak at  $\omega_{\text{LSPR}}$ , the frequency at which the condition  $\epsilon_1 + 2n_d^2 = 0$  is met. In our samples the LSPR peak occurs

at  $\sim 402$ , 410, and 412 nm for the 3 Ag, 4.5 Ag, and 6 Ag samples, respectively.

For metal nanocrystals there are additional effects that can cause shifting of the SPR peak position. From effective medium theory, the LSPR frequency can be shifted by changing the index of refraction of the host  $n_d$  or by changing the dielectric function of the metal.<sup>13</sup> For Ag particles greater than 5–10 nm in diameter, the dielectric functions of the metal are expected to approach that of the bulk metal.<sup>15,16</sup> In this regime the extinction is dominated by the dipole absorption term for particles less than  $\sim 25$  nm in diameter with scattering becoming increasingly important as the diameter increases as will be discussed below.<sup>16</sup> Particle-size distribution can also impact the peak position as well as the magnitude and the full width at half maximum of the SPR,<sup>17</sup> with a broader size distribution leading to greater absorption for all wavelengths. Larger NPs have larger absorption and scattering cross sections than the smaller NPs. Thus larger particles dominate the optical properties of the composite provided that the frequency of distributions of large and small particles is comparable. For particles larger than  $>25$  nm in diameter (not the case here), higher-order multipole terms may be necessary to describe the extinction behavior and produce additional LSPR peaks.<sup>16</sup> If the particles are sufficiently close, NP-NP interactions can also result in an additional peak in the absorption spectra.<sup>18</sup>

Based on the size of Ag NPs observed in the TEM micrographs (Fig. 2), we expect the position of the surface plasmon resonance to redshift as the Ag nanocrystal size increases,<sup>17,19</sup> provided there are no significant NP-NP interactions. The redshift of the LSPR in our samples is then attributed to the increasing size of the nanoparticles as the dose increases from  $3 \times 10^{16}$  to  $6.0 \times 10^{16}$  ions/cm<sup>2</sup>. The 3 Ag, 4.5 Ag, and 6 Ag samples have the characteristic surface plasmon resonance absorption for Ag NPs at  $\sim 402$ , 410, and 412 nm, respectively [Figs. 3(a)–3(c)].<sup>9,14,20</sup> Since the size of the NPs observed in these samples is not large enough for higher-order multipoles to contribute significantly,<sup>13,15,21</sup> we attribute the shoulder at  $\sim 524$  nm to a dipole-dipole interaction between the large Ag nanocrystals within the layer of larger particles.<sup>18,21</sup>

In the IF reflectance spectra, a single peak is observed in the 3 Ag sample at 370 nm. For the 4.5 Ag and 6 Ag samples, IF reflectance spectra of two peaks, 370 and 439 nm in the 4.5 Ag sample and at 365 and 449 nm in the 6 Ag sample, are observed. Nistor *et al.*<sup>2</sup> reported a redshift and broadening of the reflectance peaks as the NPs grow in size. Here we observe a similar redshift with increasing dose and increasing particle size for the second longer-wavelength peak, which more closely mimics the wavelength of the peaks observed. They did not observe the lower wavelength peaks, though they did note the possibility of such a second peak. We discuss below possible reasons why this second peak was not observed.

For the NIF reflectance spectra, only one peak in each sample is observed at 384, 404, and 398 nm, respectively, for the 3 Ag, 4.5 Ag and 6 Ag samples. These peaks are clearly

redshifted from the shortest wavelength peak seen in the IF reflectance spectra. This redshift has also been reported by Nistor *et al.*<sup>2</sup>

From the TEM results (Fig. 2) the majority of the small (diameter  $d$  less than 10 nm) Ag nanoparticles are located nearer the surface of the implanted side, whereas larger ( $>10$  nm) nanoparticles are farther from the surface in the 4.5 Ag and 6 Ag samples. Relatively few small NPs ( $<10$  nm) are seen to be located deeper than the larger particles. As the particles grow the scattering coefficient increases while the absorption coefficient decreases.<sup>22</sup> For NPs with radii of less than 10 nm, the ratio of absorption efficiency to scattering efficiency at 400 nm is  $>2$ ; as the wavelength increases to 450 nm the ratio of absorption efficiency to scattering efficiency drops to less than 1.5. With increasing particle size, the scattering coefficient becomes a factor of 4 larger than the absorption efficiency at 400 nm and a factor of 5 larger at 450 nm.<sup>18</sup>

If the incident beam hits the IF surface first for wavelengths less than 350 nm, the smaller particles first scatter and absorb the light before it strikes the larger NPs. As the wavelength of illumination increases the scattering also increases. As the LSPR is approached the absorption becomes larger, driving down the reflected light and the first peak is formed. This is observed in the IF spectra as the dip between the peaks is at the approximate maximum of the absorption [Figs. 3(a)–3(c)]. As the scanning wavelength continues to increase, the small particles do not absorb or scatter very well and the longer wavelength light gets to the large particles deeper in the sample with a higher intensity than at the shorter wavelengths. The absorption and scattering are significantly larger for these particles. The larger NPs are more efficient scatterers and a second peak appears, corresponding to the region where their scattering is more efficient than the absorption. This explains why, after the absorption at SPR wavelength of  $\sim 402$ – $412$  nm, the absorption drops off rapidly for the longer wavelengths. As the wavelength continues to increase, scattering efficiencies drop rapidly and the second absorption peak is formed.

Now if we illuminate the NIF, the absorption and scattering for the larger NPs dominate even at shorter wavelengths; thus the reflection spectra for the NIF are much broader than both peaks in the IF spectra. The single peak in the NIF spectrum has approximately the same width as the two peaks in the IF spectrum, as would be expected if absorption and scattering are dominated by large NPs that are seen by the scanning light first when illuminating from the NIF.

As the larger NPs scatter and absorb more strongly for all wavelengths than smaller NPs, when the reflectance is measured from the NIF, the larger nanoparticles are dominant and the light is scattered or absorbed before reaching the smaller nanoparticles where a significant portion would be absorbed instead of scattered.

If the NPs are similar in size, as in the 3 Ag sample, the reflection is more balanced between IF and NIF illumination, and there is insufficient asymmetry in particle size to produce the double peaks. In general, due to the approximately Gaussian distribution of implanted ions, a band containing

larger NPs is formed due to the higher concentration of implanted ions.<sup>23</sup> For the  $3 \times 10^{16}$  Ag implanted sample, where there are indications of the second peak in the IF spectra, the effect is less pronounced because the particles are not as disparate in size. As a result we only observe a single peak in IF or NIF spectra for this sample.

Shoulders are observed in the spectra of the 6 Ag sample at  $\sim 502$  nm in the IF spectra and at  $\sim 503$  nm in the NIF spectra. In absorption spectra, this shoulder has been attributed to dipole-dipole coupling.<sup>9,21</sup> Here we suggest the same type of effect in the reflection measurements and the reason for the same wavelength in the IF and NIF spectra. Based on the size of the NPs from TEM, the particle sizes are too small to support a higher order multipole term.

#### IV. CONCLUSION

The example of the Ag:SiO<sub>2</sub> NP materials shows that the shift in reflectance peak with direction of illumination requires a bimodal size distribution of particles occupying distinct depth distributions. Based on our experimental results, three conditions are necessary to observe the two peaks in the IF spectra. The first is sufficient asymmetry in particle sizes. The second is sufficient spatial separation of the Ag nanoparticles to separate light from the larger and smaller NPs in time. This would occur in low energy implanted samples below 100 keV for Ag. Nistor *et al.*<sup>2</sup> only observed *indications* of two peaks and not distinct peaks because based on their published TEM, the asymmetric nanoparticles were not sufficiently spread out to fulfill this condition for the formation of two distinct peaks. The third condition arises because the source terms for the two reflection peaks depend strongly on the interplay of the scattering and absorption efficiencies and their wavelength dependence. Based on the calculated scattering and absorption coefficients, Au and Cu may be possible candidates under appropriate size conditions. In the case of Cu we estimate the size differences would have to range from 5 to 80 nm to achieve a strong effect. Cu NPs have an additional problem in that CuO can form a thin shell on the surface of the NPs, greatly altering the scattering efficiency of the metallic Cu NPs. For Au, on the other hand, particle size would need to range from 5 to 40 nm or larger to achieve a noticeable effect. In the present case, this was achieved by implanting at an energy sufficient to lead to substantial straggling and the formation of a layer of smaller NPs nearer the implanted surface of the material.

It has not escaped our notice that these same conditions can be created by sputtering of a binary system comprising layers of NPs of different sizes separated by appropriate dielectric layers. Indeed, since Mie and effective-medium theories can be easily applied to such a layered structure, it should be possible to design these materials more or less from first principles. This is nicely illustrated by a Mie theory calculation shown in Fig. 4, showing the reflectance curve for a bilayer comprising of 20 and 6 nm Ag particles. Note that the “notch” in the reflectance curve due to absorption by the smaller NPs is very similar with those seen in Fig. 3. Taken together, the simulation and the experiments

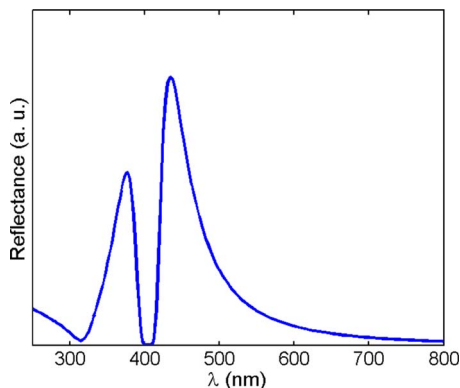


FIG. 4. (Color online) Mie simulation of the reflectance spectra for a bilayer nanocomposite with 20 and 6 nm silver nanoparticles in silica.

indicate that it should be possible to design such dichroic structures and fabricate them, for example, by multiple-target sputtering.

## ACKNOWLEDGMENTS

This research was partially supported by the U.S. Department of Energy, Office of Science (Grant No. DE-FG02-01ER45916). A.H. acknowledges research support from the National Science Foundation's GOALI program (Grant No. DMR-0513048).

<sup>1</sup>H. Tait, *5,000 Years of Glass* (H. N. Abrams, New York, 1991).

<sup>2</sup>L. C. Nistor, J. van Landuyt, J. D. Barton, D. E. Hole, N. D. Skelland, and P. D. Townsend, *J. Non-Cryst. Solids* **162**, 217 (1993).

<sup>3</sup>T. S. Anderson, R. H. Magruder III, R. A. Zuhr, and J. E. Wittig, *J.*

*Electron. Mater.* **25**, 27 (1996).

<sup>4</sup>F. Gonella, *Nucl. Instrum. Methods Phys. Res. B* **166-167**, 831 (2000).

<sup>5</sup>T. S. Anderson, R. H. Magruder III, R. A. Weeks, and R. A. Zuhr, *J. Non-Cryst. Solids* **203**, 114 (1996).

<sup>6</sup>R. H. Magruder III, R. F. Haglund, L. Yang, J. E. Wittig, and R. A. Zuhr, *J. Appl. Phys.* **76**, 708 (1994).

<sup>7</sup>A. Yelon, K. N. Piyakis, and E. Sacher, *Surf. Sci.* **569**, 47 (2004).

<sup>8</sup>M. Antonello, G. W. Arnold, G. Battaglin, R. Bertocello, E. Cattaruzza, P. Colombo, G. Mattei, P. Mazzoldi, and F. Trivillin, *J. Mater. Chem.* **8**, 457 (1998).

<sup>9</sup>R. H. Magruder III and R. A. Zuhr, *J. Appl. Phys.* **77**, 3546 (1995).

<sup>10</sup>T. S. Anderson, R. H. Magruder III, J. Wittig, D. L. Kinser, and R. A. Zuhr, *Nucl. Instrum. Methods Phys. Res. B* **171**, 401 (2000).

<sup>11</sup>J. A. Creighton and D. G. Eadon, *J. Chem. Soc., Faraday Trans.* **87**, 3881 (1991).

<sup>12</sup>U. Kreibig, M. Gartz, and A. Hilger, *Ber. Bunsenges. Phys. Chem.* **101**, 1593 (1997).

<sup>13</sup>C. Flytzanis, F. Hache, M. C. Klein, D. Ricard, and Ph. Roussignol, *Prog. Opt.* **29**, 321 (1991).

<sup>14</sup>C. F. Bohren and D. R. Huffman, *Absorption and Scattering of Light by Small Particles* (Wiley, New York, 1983).

<sup>15</sup>M. Vollmer and U. Kreibig, in *Collective Excitations in Large Metal Nanoclusters, Nuclear Physics Concepts in the Study of Atomic Cluster Physics*, edited by R. Schmidt, H. O. Lutz, and R. Dreizler (Springer, Berlin, 1992), pp. 266–276.

<sup>16</sup>U. Kreibig and M. Vollmer, *Optical Properties of Metal Nanoparticles*, Springer Series in Materials Science (Springer-Verlag, Berlin, 1995).

<sup>17</sup>G. W. Arnold and J. A. Borders, *J. Appl. Phys.* **48**, 1488 (1977).

<sup>18</sup>Z. Liu, H. Wang, H. Li, and X. Wang, *Appl. Phys. Lett.* **72**, 1823 (1998).

<sup>19</sup>D. C. Skillman and C. R. Berry, *J. Opt. Soc. Am.* **63**, 707 (1973).

<sup>20</sup>U. Kreibig and L. Genzel, *Surf. Sci.* **156**, 678 (1985).

<sup>21</sup>R. H. Magruder III and A. Meldrum, *J. Non-Cryst. Solids* **353**, 4813 (2007).

<sup>22</sup>C. R. Bamford, *Colour Generation and Control in Glass, Glass Science and Technology 2* (Elsevier, Amsterdam, 1977), p. 100.

<sup>23</sup>A. Meldrum, R. F. Haglund, L. A. Boatner, and C. W. White, *Adv. Mater. (Weinheim, Ger.)* **13**, 1431 (2001).